J. Biomechanics Vol. 21, No. 11, pp. 947–954, 1988.
Printed in Great Britain

0021-9290/88 $3.00 + .00

EFFECTS OF PERISTALTIC AND LONGITUDINAL WAVE MOTION OF THE CHANNEL WALL ON MOVEMENT OF MICRO-ORGANISMS: APPLICATION TO SPERMATOZOA TRANSPORT

J. B. SHUKLA, P. CHANDRA and RAJIV SHARMA
Department of Mathematics, I.I.T. Kanpur – 208 016, India.

and

G. RADHAKRISHNAMACHARYA
Department of Mathematics, Regional Engineering College, Warangal, India.

Abstract—A mathematical model is presented to study the motion of the spermatozoa in the cervical canal by considering the transverse waves along its tail and the transverse and longitudinal motions of the cervical wall. In an attempt to control fertility by reducing the speeed of sperm, the transverse waves have been considered in the direction opposite to the motion of the spermatozoa. It has been shown that by having appropriate transverse wave motion and longitudinal velocity, the sperm may not be able to move towards the oviduct even if it could continue to have its own propelling velocity.

A particular case of the motion of a thin plane sheet in a channel under peristaltic motion of its walls has also been obtained and studied.

INTRODUCTION

The study of swimming of micro-organisms was initiated by Taylor (1951) who modelled it as a two dimensional, infinite extensible sheet of zero thickness with a sinusoidal wave travelling down its length. Hancock (1953) studied the propulsion of a thin circular filament through a cylindrical tube for several wave amplitudes and radii of the tube. Further studies were conducted for small wave amplitudes and long wave lengths approximation by Gray and Hancock (1955), Reynolds (1965), Shack and Lardner (1974), Shack *et al.* (1974), Lighthill (1976) and others. Attempts were also made to explain the motion of spermatozoa in the female genital tract by considering the dynamical interaction of the wall (Smelser *et al.*, 1974; Shukla *et al.*, 1978). Blake *et al.* (1983) presented a theoretical model of ovum transport in the oviduct incorporating transport mechanisms due to ciliary and muscular activity of the wall by adding a force distribution term in the equation of motion. The motion due to ciliary and muscular activity can also be represented by a combination of peristaltic waves (Barton and Raynor, 1968; Shapiro *et al.*, 1969; Shack and Lardner, 1972; Guha *et al.*, 1975; Gupta and Seshadri, 1976; Shukla *et al.*, 1980) and longitudinal waves (Macagno *et al.*, 1975; Melville and Denli, 1979) along the walls.

It may be noted here that the effect of peristalsis on the motion of spermatozoa has not been studied by any of the earlier authors. In this paper, therefore, we present a mathematical model to study the motion of self propelling micro-organisms when the wall of the channel is undergoing peristaltic and longitudinal wave motion.

The main aim of the study is to apply the analysis to fertility control by reducing the speed of spermatozoa in the female genital tract. Analysis presented here, suggests that if the peristaltic waves are induced in the direction opposite to motion of the spermatozoa by some biochemical or other means, it may be possible to reduce the speed of spermatozoa to such an extent that they may not be able to reach the point of fertilization.

The other aim of this paper is to study the motion of a thin sheet in a channel when travelling peristaltic waves are imposed on the walls of the channel.

MATHEMATICAL MODEL

Consider the swimming of a thin propelling sheet in a Newtonian incompressible fluid flowing through a two-dimensional channel having flexible boundaries. It is assumed that the sheet, while swimming, sends down lateral waves of finite amplitude along its length. Further, peristaltic waves of finite amplitude are imposed along the flexible walls of the channel in the direction opposite to the motion of the sheet as shown in Fig. 1. The sheet is considered to be swimming with a propulsive velocity V_p' in the negative axial direction. It is assumed that the waves travelling along the channel walls and along the sheet are in synchronization under steady state and thus have the same wave speed C (along positive axial direction) and wavelength λ. In a fixed frame of reference (X', Y', t') the

Received 11 *August* 1986.

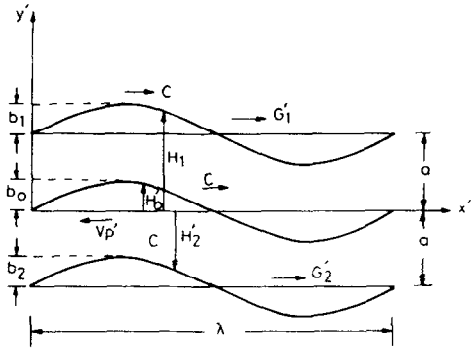

Fig. 1. Propagation of an elastic sheet swimming through a two-dimensional channel with peristaltic and longitudinal motion of walls.

shapes of the walls and the sheet at an instant t' are given by,

$$H_1'(X', t') = a + b_1 \sin\frac{2\pi}{\lambda}(X' - Ct' + V_p't') \tag{1}$$

$$H_2'(X', t') = -a + b_2 \sin\frac{2\pi}{\lambda}(X' - Ct' + V_p't') \tag{2}$$

$$H_0'(X', t') = b_0 \sin\frac{2\pi}{\lambda}(X' - Ct + V_p't') \tag{3}$$

where b_1, b_2 are the amplitudes of the peristaltic waves travelling along the upper wall and the lower wall respectively, $2a$ is the width of the channel and b_0 is the amplitude of the lateral wave along the sheet.

Since the Reynolds number involved in the swimming of a microorganism is of the order of 10^{-3}, the governing equations for fluid flow can be written, after neglecting the inertia terms, as follows

$$-\frac{\partial p'^{\pm}}{\partial X'} + \mu\left[\frac{\partial^2 U'^{\pm}}{\partial X'^2} + \frac{\partial^2 U'^{\pm}}{\partial Y'^2}\right] = 0 \tag{4}$$

$$-\frac{\partial p'^{\pm}}{\partial Y'} + \mu\left[\frac{\partial^2 V'^{\pm}}{\partial X'^2} + \frac{\partial^2 V'^{\pm}}{\partial Y'^2}\right] = 0 \tag{5}$$

$$\frac{\partial U'^{\pm}}{\partial X'} + \frac{\partial V'^{\pm}}{\partial Y'} = 0 \tag{6}$$

where U', V' are the velocity components along the X' and Y' directions respectively, p' is the pressure, μ is the viscosity of the fluid and $(\pm)$ refer to various quantities in the regions $(H_0' \leqslant Y' \leqslant H_1')$ and $(H_2' \leqslant Y' \leqslant H_0')$ respectively.

Taking into account the longitudinal motility of the walls, the boundary conditions are

$$\left.\begin{aligned} U'^{+}(X', t') &= G_1'(X' - Ct + V_p't') \\ V'^{+}(X', t') &= \frac{\partial H_1'}{\partial t'} \end{aligned}\right\} \text{at } Y' = H_1'(X', t') \tag{7}$$

$$\left.\begin{aligned} U'^{-}(X', t') &= G_2'(X' - Ct' + V_p't') \\ V'^{-}(X', t') &= \frac{\partial H_2'}{\partial t'} \end{aligned}\right\} \text{at } Y' = H_2'(X', t') \tag{8}$$

$$\left.\begin{aligned} U'^{+}(X', t') &= U'^{-}(X', t') = -V_p' \\ V'^{+}(X', t') &= V'(X', t') = \frac{\partial H_0'}{\partial t'} \end{aligned}\right\} \text{at } Y' = H_0'(X', t') \tag{9}$$

where G_1' and G_2' represent the total longitudinal velocity of the walls.

Further the sheet is self-propelling and the forces exerted by the fluid on it must balance for its motion with a constant velocity, i.e.

$$\int_S (T^+ + T^-)dS = 0 \tag{10}$$

where T^+ and T^- are the resultant of forces acting on the upper and lower surfaces of the sheet respectively and S is the surface area of the micro-organism.

In a frame (x', y', t') moving with velocity $C - V_p'$ in the positive axial direction, the sheet and the walls of the channel appear stationary and the flow in this moving frame will be steady.

Using the following transformation

$$x' = X' - Ct' + V_p't'; \quad y' = Y' \tag{11}$$

and introducing the following dimensionless quantities

$$x = x'/\lambda, \quad y = y'/a, \quad t = Ct'/\lambda,$$

$$p = p'\Big/\frac{\mu C\lambda}{a^2}, \quad v^{\pm} = V'^{\pm}\Big/\frac{Ca}{\lambda}$$

$$(u^{\pm}, V_p, g_i) = (U'^{\pm}, V_p', G_i')/C, \quad i = 1, 2$$

$$h_i = H_i'/a, \quad \varepsilon_i = b_i/a, \quad i = 0, 1, 2.$$

Equations (4, 5, and 6) under long wavelength approximation $(a/\lambda \ll 1)$, get reduced to

$$-\frac{\partial p^{\pm}}{\partial x} + \frac{\partial^2 u^{\pm}}{\partial y^2} = 0 \tag{12}$$

$$-\frac{\partial p^{\pm}}{\partial y} = 0 \tag{13}$$

$$\frac{\partial u^{\pm}}{\partial x} + \frac{\partial v^{\pm}}{\partial y} = 0. \tag{14}$$

The boundary conditions for u are written in dimensionless form as

$$\left.\begin{aligned} u^{+} &= V_p + g_1(x) - 1 = U_1; && y = h_1(x) \\ u^{-} &= V_p + g_2(x) - 1 = U_2; && y = h_2(x) \\ u^{+} &= u^{-} = -1; && y = h_0(x) \end{aligned}\right\} \tag{15}$$

where

$$\left.\begin{aligned} h_0(x) &= \varepsilon_0 \sin 2\pi x \\ h_1(x) &= 1 + \varepsilon_1 \sin 2\pi x \\ h_2(x) &= -1 + \varepsilon_2 \sin 2\pi x. \end{aligned}\right\} \tag{15a}$$

Further using the stress-strain relationship and using long wavelength approximation, the force equilibrium condition (10) can be written as

$$\int_0^1 [p]\,dx = 0 \tag{16}$$

$$\int_0^1 \left(\left[\frac{\partial u}{\partial y} \right]_{y=h_0(x)} + \frac{dh_0}{dx}[p] \right) dx = 0 \tag{17}$$

where $[f]$ indicates the difference in the quantity f above and below the sheet.

MATHEMATICAL ANALYSIS

The differential equation (12) is solved with boundary conditions (15) to obtain the velocities u^+ and u^- in the regions $(h_0 \leqslant y \leqslant h_1)$ and $(h_2 \leqslant y \leqslant h_0)$ respectively, which are given as follows

$$u^+ = \frac{1}{2}\left(\frac{\partial p^+}{\partial x}\right)(y^2 - h_1 y - h_0 y + h_1 h_0) + U_1 \frac{(y-h_0)}{(h_1-h_0)} - \frac{(h_1-y)}{(h_1-h_0)} \tag{18}$$

$$u^- = \frac{1}{2}\left(\frac{\partial p^-}{\partial x}\right)(y^2 - h_2 y - h_0 y + h_0 h_2) + U_2 \frac{(y-h_0)}{(h_2-h_0)} - \frac{(h_2-y)}{(h_2-h_0)}. \tag{19}$$

The dimensionless flow flux $q^{\pm}(=q'^{\pm}/aC)$ in the moving frame can be obtained as

$$q^+ = \int_{h_0}^{h_1} u^+\,dy \quad \text{and} \quad q^- = \int_{h_2}^{h_0} u^-\,dy$$

which on using equations (18) and (19) gives

$$q^+ = -\frac{1}{12}\left(\frac{\partial p^+}{\partial x}\right)(h_1-h_0)^3 + \tfrac{1}{2}(h_1-h_0)(U_1-1) \tag{20}$$

$$q^- = -\frac{1}{12}\left(\frac{\partial p^-}{\partial x}\right)(h_0-h_2)^3 + \tfrac{1}{2}(h_0-h_2)(U_2-1). \tag{21}$$

To obtain the pressure gradients $\partial p^{\pm}/\partial x$, the equations (20) and (21) can be rewritten as

$$\frac{\partial p^+}{\partial x} = -12\frac{q^+}{(h_1-h_0)^3} + 6\frac{U_1-1}{(h_1-h_0)^2} \tag{22}$$

$$\frac{\partial p^-}{\partial x} = -12\frac{q^-}{(h_0-h_2)^3} + 6\frac{U_2-1}{(h_0-h_2)^2}. \tag{23}$$

Integrating the equation of continuity (14), it can be seen that the two fluxes $q^{\pm}$ are constants. Further it is evident that Δp, the pressure rise over a wavelength is same for the two regions.

Integrating equations (22) and (23) over a wavelength, we get the following two relations among the three unknown quantities V_p, q^+ and q^-

$$-12q^+ I_{11} + 6V_p I_{12} + 6I_{13} - 12I_{12} = \Delta p \tag{24}$$

$$-12q^- I_{21} + 6V_p I_{22} + 6I_{23} - 12I_{22} = \Delta p. \tag{25}$$

Using the expressions (18), (19) and (22), (23) for $u^{\pm}$ and $\partial p^{\pm}/\partial x$, the force equilibrium condition (17) provides us with the third relationship necessary to determine V_p, q^+ and q^- as

$$12q^+ I_{31} - 12q^- I_{32} + 2V_p I_{33} + 2(I_{34} + I_{35}) - 12I_{36} = 2\Delta p \tag{26}$$

where

$$I_{i1} = (-1)^i \int_0^1 \frac{dx}{(h_0-h_i)^3}; \quad I_{i2} = \int_0^1 \frac{dx}{(h_0-h_i)^2};$$

$$I_{i3} = \int_0^1 \frac{g_i(x)\,dx}{(h_0-h_i)^2}, \quad i = 1, 2 \tag{27}$$

and

$$I_{31} = \int_0^1 \frac{h_1+h_0-1}{(h_1-h_0)^3}dx$$

$$I_{32} = \int_0^1 \frac{h_2+h_0+1}{(h_0-h_2)^3}dx$$

$$I_{33} = \int_0^1 \left[\frac{3-2h_1-4h_0}{(h_1-h_0)^2} + \frac{3+2h_2+4h_0}{(h_0-h_2)^2}\right]dx$$

$$I_{34} = \int_0^1 \left[\frac{3-2h_1-4h_0}{(h_1-h_0)^2}\right] g_1(x)dx \tag{28}$$

$$I_{35} = \int_0^1 \left[\frac{3+2h_2+4h_0}{(h_0-h_2)^2}\right] g_2(x)dx$$

$$I_{36} = \int_0^1 \left[\frac{1-h_1-h_0}{(h_1-h_0)^2} + \frac{1+h_2+h_0}{(h_0-h_2)^2}\right]dx.$$

Solving equation (24)–(26) we get

$$V_p = \frac{\left[\left(2 + \frac{I_{31}}{I_{11}} - \frac{I_{32}}{I_{21}}\right)\Delta p - 2I_{34} - 2I_{35} + 12I_{36} - \frac{I_{31}}{I_{11}}I_{41} + \frac{I_{32}}{I_{21}}I_{42}\right]}{\left[2I_{33} + 6\frac{I_{31}}{I_{11}}I_{12} - 6\frac{I_{32}}{I_{21}}I_{22}\right]} \tag{29}$$

where, $I_{41} = 6(I_{13} - 2I_{12})$ and $I_{42} = 6(I_{23} - 2I_{22})$ and the total flux $q = q^+ + q^-$ is

$$q = -\left(\frac{1}{I_{11}} + \frac{1}{I_{21}}\right)\frac{\Delta p}{12} + \left(\frac{I_{12}}{I_{11}} + \frac{I_{22}}{I_{21}}\right)\frac{V_p}{2} + \left(\frac{I_{13}-2I_{12}}{2I_{11}} + \frac{I_{23}-2I_{22}}{2I_{21}}\right). \tag{30}$$

The flux in the stationary frame Q is related to the flux q in the moving frame by the following relationship

$$Q=q+(1-V_p)(H_2-H_1)/a. \tag{31}$$

Averaging equation (31) over a time period we therefore get the time averaged flow $\bar{Q}$ in terms of q and V_p as

$$\bar{Q}=q+2(1-V_p). \tag{32}$$

Equations (29), (30) and (32) provide expressions for V_p, q and $\bar{Q}$ for the given forms of $h_0(x)$, $h_1(x)$, $h_2(x)$ [15(a)] and general forms of functions $g_1(x)$, $g_2(x)$ representing the longitudinal motility of the channel. In the following analysis we consider the following forms of longitudinal motion of the wall

$$\begin{aligned} g_1(x)&=C_{11}+C_{12}\sin 2\pi x \\ g_2(x)&=C_{21}+C_{22}\sin 2\pi x. \end{aligned} \tag{33}$$

For these given forms of h_0, h_1, h_2 and g_1, g_2 and writing

$$\alpha_1=\varepsilon_1-\varepsilon_0,\ \alpha_2=\varepsilon_0-\varepsilon_2. \tag{34}$$

The expressions (27) and (28) reduce to

$$\begin{aligned} I_{i1}&=\int_0^1 \frac{dx}{(1+\alpha_1\sin 2\pi x)^3} \\ I_{i2}&=\int_0^1 \frac{dx}{(1+\alpha_i\sin 2\pi x)^2} \quad (i=1,2) \\ I_{i3}&=C_{i1}I_{i2}+C_{i2}I_{i4} \\ I_{i4}&=\int_0^1 \frac{\sin 2\pi x}{(1+\alpha_i\sin 2\pi x)^2} \end{aligned} \tag{35}$$

and

$$\begin{aligned} I_{31}&=(\varepsilon_0+\varepsilon_1)\int_0^1 \frac{\sin 2\pi x}{(1+\alpha_i\sin 2\pi x)^3}dx \\ I_{32}&=(\varepsilon_0+\varepsilon_2)\int_0^1 \frac{\sin 2\pi x}{(1+\alpha_2\sin 2\pi x)^3}dx \\ I_{33}&=I_{12}-2(\varepsilon_1+2\varepsilon_0)I_{14}+I_{22}+2(\varepsilon_2+2\varepsilon_0)I_{24} \\ I_{34}&=[I_{12}-2(\varepsilon_1+2\varepsilon_0)I_{14}]C_{11} \\ &\quad+[I_{14}-2(\varepsilon_1+2\varepsilon_0)I_{37}]C_{12} \\ I_{35}&=[I_{22}+2(\varepsilon_2+2\varepsilon_0)I_{24}]C_{21} \\ &\quad+[I_{24}+2(\varepsilon_2+2\varepsilon_0)I_{38}]C_{22} \\ I_{36}&=-(\varepsilon_1+\varepsilon_0)I_{14}+(\varepsilon_2+\varepsilon_0)I_{24} \\ I_{37}&=\int_0^1 \frac{\sin^2 2\pi x}{(1+\alpha_1\sin 2\pi x)^2}dx. \\ I_{38}&=\int_0^1 \frac{\sin^2 2\pi x}{(1+\alpha_2\sin 2\pi x)^2}dx. \end{aligned} \tag{36}$$

These integrals can be evaluated by contour integration and are listed in Appendix A.

When there is no peristaltic motion of the walls, we have

$$\alpha_1=-\varepsilon_0,\quad \alpha_2=\varepsilon_0$$

and therefore we get the expressions for V_p, q and $\bar{Q}$ from equations (29), (30), (32) in the following simplified form

$$V_p=\frac{1}{M_0}(M_1\Delta p+M_2) \tag{37}$$

$$\begin{aligned} q=&\frac{1}{6}\Delta p\left(-\frac{1}{I_{11}}+\frac{6M_1}{M_0}\frac{I_{12}}{I_{11}}\right)+\frac{M_2}{M_0}\left(\frac{I_{12}}{I_{11}}\right) \\ &+\frac{1}{2I_{11}}[I_{12}(C_{11}+C_{21}) \\ &+I_{14}(C_{12}-C_{22})-4I_{12}] \end{aligned} \tag{38}$$

$$\begin{aligned} \bar{Q}=&\frac{1}{6}\Delta p\left(-\frac{1}{I_{11}}+6\frac{M_1}{M_0}\frac{I_{12}}{I_{11}}-12\frac{M_1}{M_0}\right) \\ &+\frac{M_2}{M_0}\left(\frac{I_{12}}{I_{11}}-2\right)+2+\frac{1}{2I_{11}}[I_{12}(C_{11}+C_{21}) \\ &+I_{14}(C_{12}-C_{22})-4I_{12}] \end{aligned} \tag{39}$$

where

$$\begin{aligned} M_0&=4I_{12}-16\varepsilon_0 I_{14}+12\frac{I_{31}}{I_{11}}I_{12} \\ M_1&=2+2\frac{I_{31}}{I_{11}} \\ M_2&=-2(I_{12}-4\varepsilon_0 I_{14})(C_{11}+C_{21}) \\ &\quad-2(I_{14}-4\varepsilon_0 I_{37})(C_{12}-C_{22}) \\ &\quad-24\varepsilon_0 I_{14}-6\frac{I_{31}}{I_{11}}[I_{12}(C_{11}+C_{21}) \\ &\quad+I_{14}(C_{12}-C_{22})-4I_{12}]. \end{aligned} \tag{40}$$

Further, if longitudinal motion is also absent i.e.

$$g_1(x)=0,\ g_2(x)=0$$

equations (37)–(39) reduce to the following forms after using the values of the integrals given in Appendix A

$$\begin{aligned} V_p&=\tfrac{1}{2}(1-\varepsilon_0^2)^{1/2}\Delta p+\frac{3\varepsilon_0^2}{1+2\varepsilon_0^2} \\ q&=\tfrac{1}{3}(1-\varepsilon_0^2)^{3/2}\Delta p-\frac{2(1-\varepsilon_0^2)}{1+2\varepsilon_0^2} \\ \bar{Q}&=-\tfrac{1}{3}(2+\varepsilon_0^2)(1-\varepsilon_0^2)^{1/2}\Delta p. \end{aligned} \tag{41}$$

These expressions are the same as those obtained by Shack and Lardner (1974) for $q=2Q$ and $\bar{Q}=2Q_F$.

DISCUSSION

The values of V_p and $\bar{Q}$ have been computed using equations (29)–(32) for the following set of parameters

$$\begin{gathered} C_{11}=0,\ C_{21}=0,\ C_1(=C_{12})=(0, 0.2, -0.2) \\ C_2(=C_{22})=(0, 0.2, -0.2) \\ \varepsilon_1=(0, 0.35),\ \varepsilon_2=(0, 0.25, -0.25), \\ \Delta p=(0, 0.05, -0.05) \end{gathered}$$

and are plotted in Figs 2–13 as functions of ε_0.

Effects of various parameters on V_p are graphically shown in Figs 2–7. In Fig. 2 the results are shown corresponding to the particular case when there is no peristaltic motion on the walls ($\varepsilon_1 = 0$, $\varepsilon_2 = 0$). As noted in the expressions (37)–(40) the velocity amplitudes $C_1 (= C_{12})$ and $C_2 (= C_{22})$ appear always as their difference $C_2 - C_1 = d$. The effect of this parameter d is, therefore, shown for $\Delta p = 0, 0.05$. It is observed that V_p increases as magnitude of ε_0 increases. For fixed $\varepsilon_0 > 0$, $V_p > 0$, V_p decreases as d increases and for $\varepsilon_0 < 0$, a reverse trend is noticed. It is also noted that, in this particular case, there is no effect of the longitudinal velocities C_1, C_2 if $\varepsilon_0 = 0$. The effect of p, for fixed values of ε_0 and d is to increase V_p.

Effect of C_1 and C_2 for non-zero values of ε_1, ε_2 is shown in Fig. 3 for $\Delta p = 0$. The effect of C_1 and C_2 is

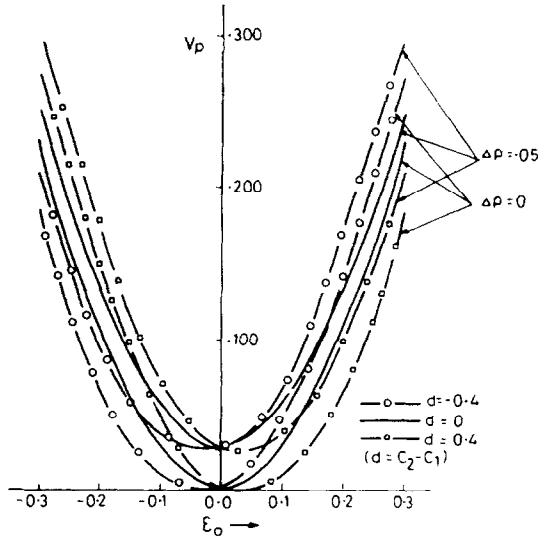

Fig. 2. Effect of C_1 and C_2 on V_p for zero ε_1 and ε_2 (no peristalsis).

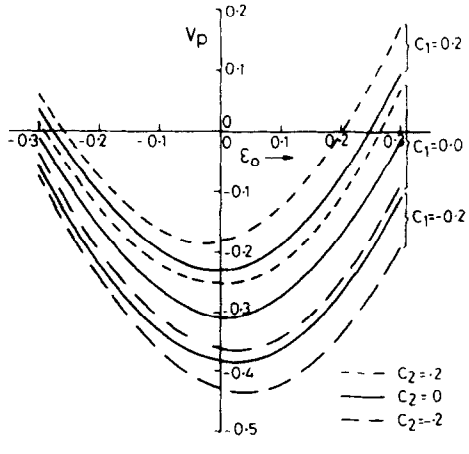

Fig. 3. Effect of C_1 and C_2 on V_p for fixed ε_1 and ε_2. ($\varepsilon_1 = 0.35$, $\varepsilon_2 = 0.25$ and $\Delta p = 0$).

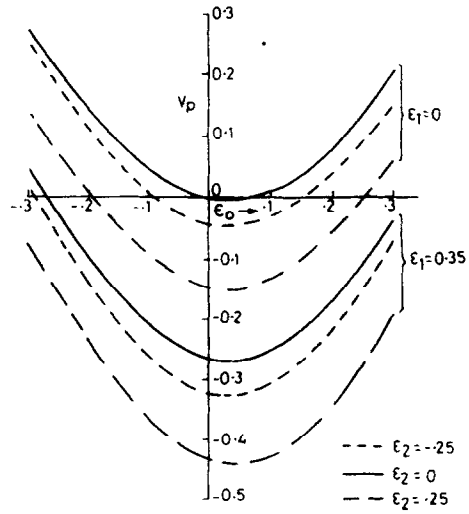

Fig. 4. Effect of ε_1 and ε_2 on V_p ($C_1 = -0.2$, $C_2 = 0.2$, $\Delta p = 0$).

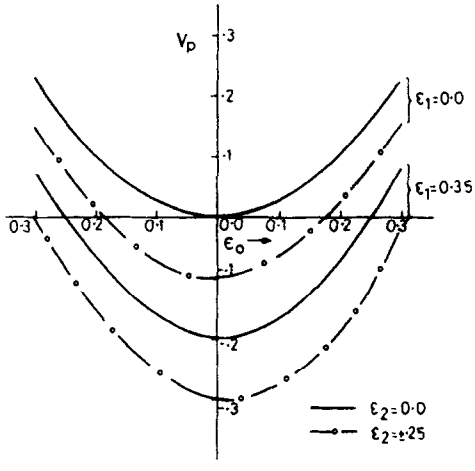

Fig. 5. Effect of ε_1 and ε_2 on V_p ($C_1 = 0$, $C_2 = 0$, $\Delta p = 0$).

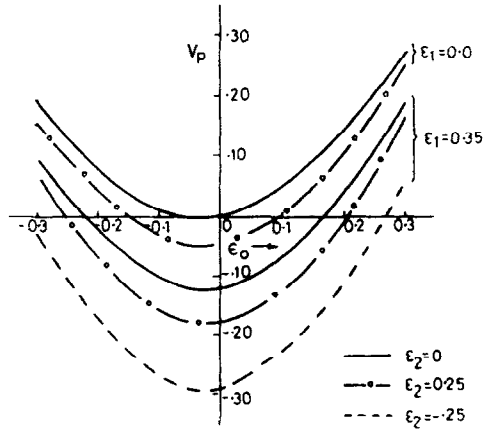

Fig. 6. Effect of ε_1 and ε_2 on V_p ($C_1 = 0.2$, $C_2 = -0.2$, $\Delta p = 0$).

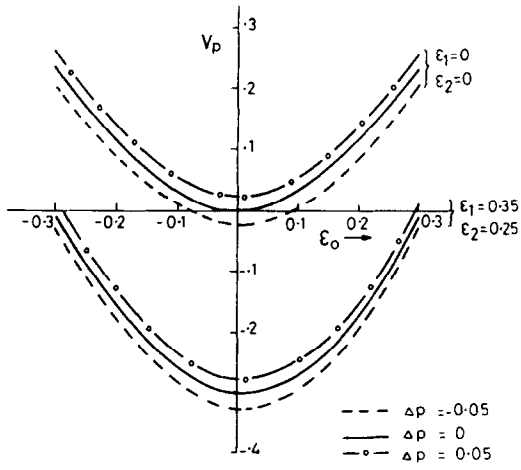

Fig. 7. Effect of Δp and ε_1, ε_2 on V_p ($C_1=0$, $C_2=0$).

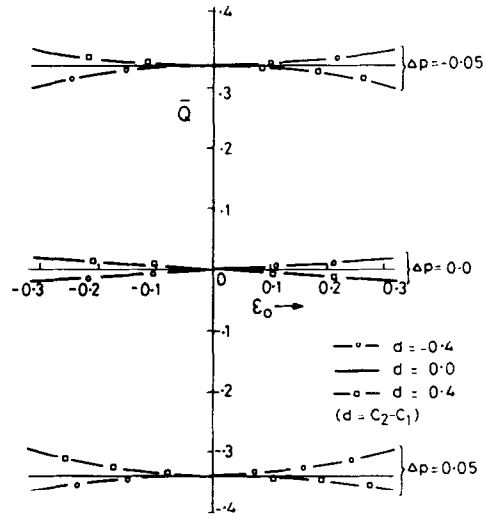

Fig. 8. Effect of C_1 and C_2 on $\bar{Q}$ for zero ε_1 and ε_2 (no peristalsis).

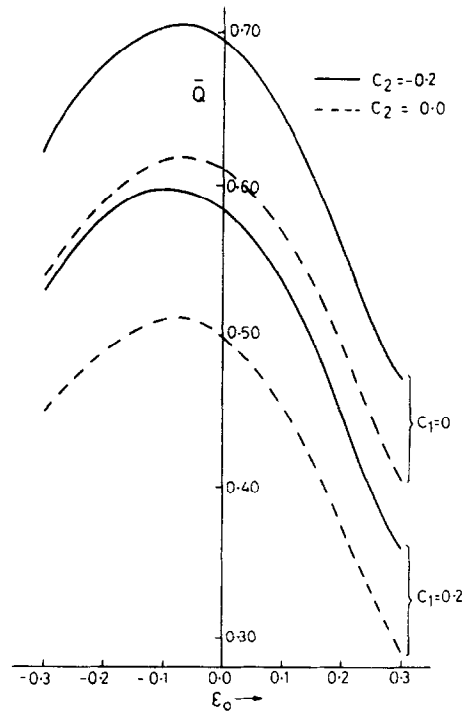

Fig. 9. Effect of C_1 and C_2 on $\bar{Q}$ ($\varepsilon_1=0.35$, $\varepsilon_2=-0.25$, $\Delta p=0$).

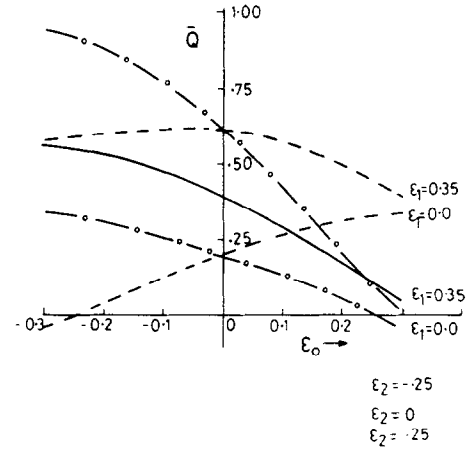

Fig. 10. Effect of ε_1 and ε_2 on $\bar{Q}$ ($C_1=0$, $C_2=0$, $\Delta p=0$.).

similar to that observed in Fig. 2. Comparing Figs 2 and 3, it can also be noticed that because of the peristalsis on the walls, the propagation velocity V_p is reduced and in fact is in the opposite direction. The maximum negative value of V_p is obtained for the combination $C_1<0$, $C_2>0$.

Similar effects of ε_1, ε_2, C_1 and C_2 can be seen from Figs 4–6, where effects of ε_1 and ε_2 are shown for fixed $(C_1, C_2)=[(-0.2, 0.2), (0, 0), (0.2, -0.2)]$ and $\Delta p=0$. Comparing these three figures it can be observed that for $C_1=C_2=0$, sign of ε_2 does not matter. The maximum negative value of V_p for fixed ε_0, ε_1 is obtained for the first case ($C_1<0$, $C_2>0$) with $\varepsilon_2>0$ (Fig. 4). An increase in Δp, the pressure rise, causes an increase in V_p (Fig. 7).

Effects of various parameters on time-average flux $\bar{Q}$ are shown in Figs 8–13. It can be seen that in general the results are opposite to those obtained for V_p. The effect of peristaltic waves on the wall is to increase $\bar{Q}$ but increase in the magnitude of the amplitude ε_0 causes a decrease in $\bar{Q}$, (Figs 8, 10, 11). It also increases as Δp becomes negative, (Figs 12, 13). For a particular case of no peristalsis ($\varepsilon_1=\varepsilon_2=0$) the effect of d is opposite to that of V_p i.e. $\bar{Q}$ is minimum for $d>0$, (Fig. 8). However in general, the maximum values of $\bar{Q}$ are obtained when C_1 and C_2 are both negative (Fig. 9).

In the following passage we apply these discussions in the study of the motion of spermatozoa in the cervix.

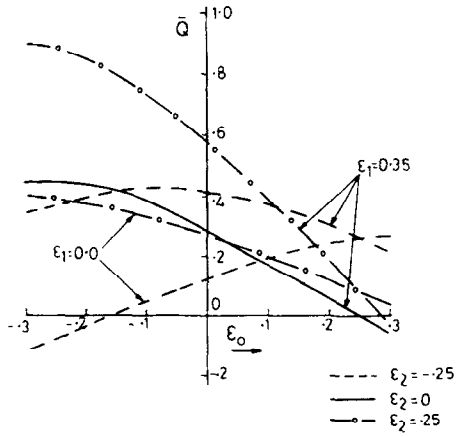

Fig. 11. Effect of ε_1 and ε_2 on $\bar{Q}$ ($C_1 = 0.2, C_2 = -0.2, \Delta p = 0$).

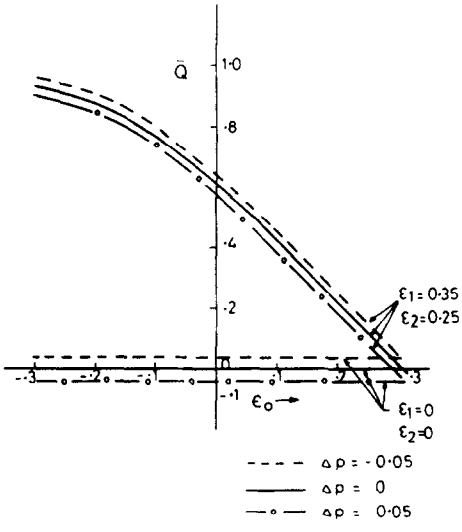

Fig. 12. Effect of Δp on $\bar{Q}$ ($C_1 = 0$, $C_2 = 0$).

APPLICATION TO SPERMATOZOA TRANSPORT: AN APPROACH TO FERTILITY CONTROL

The spermatozoa are male reproductive cells. They are specialized cells containing only 23 out of the full 46 chromosomes of a normal cell in human body. During coitus, the spermatozoa are deposited, at the time of ejaculation, at the mouth of the cervix in the female genital tract. It has been found that they take an average of 45 min to reach the fertilization point in the fallopian tube and thus travel with an average speed of 1–3 mm min^{-1}. It is necessary, from the point of fertility control, to reduce this speed of spermatozoa in the female genital tract by some biochemical or other means.

It is known that spermatozoa, when in large numbers and close to each other, travel in unison. It is therefore possible to approximate their motion by a sheet flowing through fluid (Taylor, 1951). The proposed model and results discussed earlier can therefore be applied to study the effects of peristaltic and longitudinal motion of the walls of the female genital tract on spermatozoa transport.

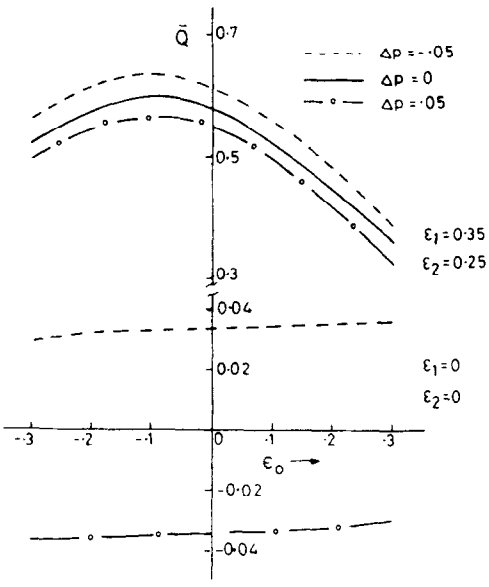

Fig. 13. Effect of Δp on $\bar{Q}$ ($C_1 = 0.2$, $C_2 = -0.2$).

Noting the effects of various parameters on V_p, as discussed earlier, it is evident that V_p can be made negative by application of a negative Δp (i.e. pressure drop) and this effect can be further enhanced by inducing the peristaltic waves travelling along the walls in the direction away from the point of fertilization. Further, the motion of the cilia can also enhance this effect by a suitable choice of longitudinal wave. It is therefore suggested that if the generation of a pressure drop and the peristaltic motion is possible by some mechanism, such as sudden withdrawal of the male organ from the vagina immediately after ejaculation, it may be possible to reduce the motion of the spermatozoa and hence controlling fertility. Thus the ancient belief behind the practice of withdrawal of the male organ immediately after ejaculation to control fertility, may have a scientific basis as predicted by this model.

A PARTICULAR CASE: MOTION OF A THIN SHEET IN A CHANNEL UNDER PERISTALTIC MOTION OF THE WALLS

This case can be obtained from the present model when there are no lateral waves on the sheet and no longitudinal wave motion along the channel walls. It should be noted that this case is physically different from the usual peristaltic flow in a channel (Shapiro *et al.*, 1969) as there exists a sheet in the middle of the channel which divides it into two separate zones.

Mathematically, this case is obtained by putting $g_1(x) = 0$, $g_2(x) = 0$ and $\varepsilon_0 = 0$ into equations (29)–(32) and then the expressions for V_p, q and $\bar{Q}$ become (for

the symmetric case when $\varepsilon_1 = -\varepsilon_2 = \varepsilon$)

$$V_p = \frac{1}{M_0}(M_1 \Delta p + M_2)$$

$$q = \frac{1}{6}\Delta p\left(-\frac{1}{I_{11}} + 6\frac{M_1 I_{12}}{M_0 I_{11}}\right) + \left(-2\frac{I_{12}}{I_{11}} + \frac{M_2 I_{12}}{M_0 I_{11}}\right) \tag{42}$$

$$\bar{Q} = \frac{1}{6}\Delta p\left(\frac{1}{I_{11}} + 6\frac{M_1 I_{12}}{M_0 I_{11}} - 12\frac{M_1}{M_0}\right) + \left(-2\frac{I_{12}}{I_{11}} + 2 + \frac{M_2 I_{12}}{M_0 I_{11}} - 2\frac{M_2}{M_0}\right)$$

where

$$M_0 = 4I_{12} - 8\varepsilon I_{14}$$

$$M_1 = 2 + 2\frac{I_{31}}{I_{11}} \tag{43}$$

$$M_2 = -24\varepsilon I_{14} + 24\frac{I_{31}}{I_{11}} I_{12}.$$

The effects of Δp, ε_1 and ε_2 on V_p and $\bar{Q}$ can be seen from Figs 2, 5, 8 and 12 for $\varepsilon_0 = 0$. It can be noted from Figs 2 and 3 that the velocity V_p of the sheet increases as Δp increases. However for $\varepsilon_1 \neq 0, \varepsilon_2 \neq 0$ it is seen that V_p is negative, i.e. the sheet flows in the direction of peristaltic waves and this effect is enhanced as ε_1 and ε_2 increase. The effects of Δp, ε_1 and ε_2 on $\bar{Q}$ can be studied from Figs 8 and 12. It is observed that $\bar{Q}$ increases as the magnitude of ε_1 and ε_2 increase and as Δp decreases.

CONCLUSION

A mathematical model to study the effect of peristaltic and longitudinal motion of the walls, on the propulsion of a sheet has been presented and the results have been applied on the swimming of spermatozoa through the female genital tract. It has been shown that the speed of spermatozoa can be reduced considerably, to avoid fertilization, by generating a pressure drop and inducing peristaltic waves on the wall of the genital tract through some biomechanical or other means such as sudden withdrawal of the male organ from the vagina immediately after ejaculation.

A particular case of the motion of a thin sheet in a channel under peristaltic motion of the walls has also been discussed. It is shown that sheet velocity is dependent on the amplitudes and direction of propagation of the peristaltic waves.

REFERENCES

Barton, C. and Raynor, S. (1968) Peristaltic flow in tubes. *Bull. math. Biophys.* **30**, 663–680.

Blake, J. R., Vann, P. G. and Winet, H. (1983) A model of ovum transport. *J. theor. Biol.* **102**, 145–166.

Gray, J. and Hancock, G. J. (1955) The propulsion of sea-urchin spermatozoa. *J. exp. Biol.* **32**, 802.

Guha, S. K., Kaur, H. and Ahmed, A. M. (1975) Mechanics of spermatic fluid transport in the vas deferens. *Med. Biol. Engng* **13**, 518–522.

Gupta, B. B. and Seshadri, V. (1976) Peristaltic pumping in non-uniform tubes. *J. Biomechanics* **9**, 105–109.

Hancock, G. J. (1953) The self propulsion of microscopic organisms through liquids. *Proc. Roy. Soc.* **217**, 96.

Lighthill, M. J. (1976) Flagellar hydrodynamics. *S.I.A.M. Rev.* **18**, 161–230.

Macagno, E., Melville, J. and Christenson, J. (1975) A model for longitudinal motility of the small intestines. *Biorheology* **12**, 369–376.

Melville, J. G. and Denli, N. (1979) Fluid mechanics of longitudinal contractions in the small intestine. *J. biomech. Engng* **101**, 284–288.

Reynolds, A. J. (1965) The swimming of minute organisms. *J. Fluid Mech.* **23**, 241–260.

Shack, W. J. and Lardner, T. J. (1972) Cilia transport. *Bull. math. Biophys.* **34**, 325–335.

Shack, W. J., Fray, C. S. and Lardner, T. J. (1974) Observations on the hydrodynamics and swimming motions of mammalian spermatozoa. *Bull. math. Biol.* **36**, 555–565.

Shack, W. J. and Lardner, T. J. (1974) A long wavelength solution for a microorganism swimming in a channel. *Bull. Math. Biol.* **36**, 435–444.

Shapiro, A. H., Jaffrin, M. Y. and Weinberg, S. L. (1969) Peristaltic pumping with long wavelengths at low Reynolds number. *J. Fluid Mech.* **37**, 799–825.

Shukla, J. B., Parihar, R. S., Rao, B. R. P. and Gupta, S. P. (1980) Effect of peripheral layer viscosity on peristaltic transport of a bio-fluid. *J. Fluid Mech.* **97**, 225–237.

Shukla, J. B., Rao, B. R. P. and Parihar, R. S. (1978) Swimming of spermatozoa in cervix: effects of dynamical interaction and peripheral layer viscosity. *J. Biomechanics* **11**, 15–19.

Smelser, R. E., Shack, W. J. and Lardner, T. J. (1974) The swimming of spermatozoa in an active channel. *J. Biomechanics* **7**, 349–355.

Taylor, G. (1951) Analysis of microscopic organisms. *Proc. R. Soc.* **209**, 447–461.

APPENDIX A.

$$\int_0^1 \frac{dx}{(1+\alpha\sin 2\pi x)} = \frac{1}{(1-\alpha^2)^{1/2}}$$

$$\int_0^1 \frac{dx}{(1+\alpha\sin 2\pi x)^2} = \frac{1}{(1-\alpha^2)^{3/2}}$$

$$\int_0^1 \frac{dx}{(1+\alpha\sin 2\pi x)^3} = \frac{2+\alpha^2}{2(1-\alpha^2)^{5/2}}$$

$$\int_0^1 \frac{dx}{(1+\alpha\sin 2\pi x)^4} = \frac{2+3\alpha^2}{2(1-\alpha^2)^{7/2}}$$

$$\int_0^1 \frac{\sin 2\pi x\, dx}{(1+\alpha\sin 2\pi x)^2} = -\frac{\alpha}{(1-\alpha^2)^{3/2}}$$

$$\int_0^1 \frac{\sin 2\pi x\, dx}{(1+\alpha\sin 2\pi x)^3} = -\frac{3\alpha}{2(1-\alpha^2)^{5/2}}$$

$$\int_0^1 \frac{\sin 2\pi x\, dx}{(1+\alpha\sin 2\pi x)^4} = \frac{5\alpha}{3(1-\alpha^2)^{7/2}} + \frac{\alpha}{3(1-\alpha^2)^{5/2}}$$

$$\int_0^1 \frac{\sin^2 2\pi x\, dx}{(1+\alpha\sin 2\pi x)^2} = \frac{1}{\alpha^2} + \frac{2\alpha^2-1}{\alpha^2(1-\alpha^2)^{3/2}}$$